Schizophrenia Bulletin Open
https://doi.org/10.1093/schizbullopen/sgae008

Current Auditory Hallucinations Are Not Associated With Specific White Matter Diffusion Alterations in Schizophrenia

Stener Nerland[1,2,*], Nora Berz Slapø[2], Claudia Barth[1,2], Lynn Mørch-Johnsen[2,3,4], Kjetil Nordbø Jørgensen[2], Dani Beck[1,5,6], Laura A. Wortinger[1,2], Lars T. Westlye[5,6], Erik G. Jönsson[2,7], Ole A. Andreassen[1,2,5], Ivan I. Maximov[5,8], Oliver M. Geier[9,10] and Ingrid Agartz[1,2,7]

[1]Department of Psychiatric Research, Diakonhjemmet Hospital, Oslo, Norway; [2]Norwegian Center for Mental Disorders Research (NORMENT), Institute of Clinical Medicine, University of Oslo, Oslo, Norway; [3]Department of Psychiatry, Østfold Hospital, Grålum, Norway; [4]Department of Clinical Research, Østfold Hospital, Grålum, Norway; [5]Norwegian Center for Mental Disorders Research (NORMENT), Division of Mental Health and Addiction, Oslo University Hospital, Oslo, Norway; [6]Department of Psychology, University of Oslo, Oslo, Norway; [7]Centre for Psychiatry Research, Department of Clinical Neuroscience, Karolinska Institutet and Stockholm Health Care Services, Stockholm Region, Stockholm, Sweden; [8]Department of Health and Functioning, Western Norway University of Applied Sciences, Bergen, Norway; [9]Department of Computational Radiology and Physics, Division of Radiology and Nuclear Medicine, Oslo University Hospital, Oslo, Norway; [10]Center for Lifespan Changes in Brain and Cognition (LCBC), Department of Psychology, University of Oslo, Oslo, Norway

[*]To whom correspondence should be addressed; University of Oslo, and Diakonhjemmet Hospital, PB 85 Vinderen, 0319 Oslo, Norway; tel: +47 22 02 99 53, e-mail: stener.nerland@medisin.uio.no

***Background and Hypothesis*: Studies have linked auditory hallucinations (AH) in schizophrenia spectrum disorders (SCZ) to altered cerebral white matter microstructure within the language and auditory processing circuitry (LAPC). However, the specificity to the LAPC remains unclear. Here, we investigated the relationship between AH and DTI among patients with SCZ using diffusion tensor imaging (DTI).*Study Design*: We included patients with SCZ with (AH+; $n = 59$) and without (AH−; $n = 81$) current AH, and 140 age- and sex-matched controls. Fractional anisotropy (FA), mean diffusivity (MD), radial diffusivity (RD), and axial diffusivity (AD) were extracted from 39 fiber tracts. We used principal component analysis (PCA) to identify general factors of variation across fiber tracts and DTI metrics. Regression models adjusted for sex, age, and age^2 were used to compare tract-wise DTI metrics and PCA factors between AH+, AH−, and healthy controls and to assess associations with clinical characteristics.*Study Results*: Widespread differences relative to controls were observed for MD and RD in patients without current AH. Only limited differences in 2 fiber tracts were observed between AH+ and controls. Unimodal PCA factors based on MD, RD, and AD, as well as multimodal PCA factors, differed significantly relative to controls for AH−, but not AH+. We did not find any significant associations between PCA factors and clinical characteristics.*Conclusions*: Contrary to previous studies, DTI metrics differed mainly in patients *without* current AH compared to controls, indicating a widespread neuroanatomical distribution. This challenges the notion that altered DTI metrics within the LAPC is a specific feature underlying AH.**

Key words: white matter microstructure/magnetic resonance imaging/probabilistic tractography/psychotic disorders/dimensionality reduction

Introduction

Auditory hallucinations (AH), ie, auditory percepts not elicited by an external source, is a core symptom in schizophrenia spectrum disorders (SCZ).[1–3] Although the pathophysiology of AH is poorly understood, magnetic resonance imaging (MRI) studies have implicated alterations in cerebral white matter (WM) microstructure,[4–7] regional morphology of the cerebral cortex,[8,9] and functional activation during active hallucination.[10] Notably, many studies report alterations in the language and auditory processing circuitry (LAPC)[11,12] in patients with SCZ and AH, including cortical regions such as Heschl's gyrus,[8] Broca's area,[13] and Wernicke's area,[14]

as well as the WM fiber tracts connecting them. It has been hypothesized that disrupted connectivity within the LAPC results in erroneous source attribution, which in turn leads to AH.[15–18]

Diffusion tensor imaging (DTI) studies have reported alterations in WM fiber tracts within the LAPC in patients with SCZ and AH.[19–22] Given its crucial role in language processing, the left arcuate fasciculus (AF), a heavily myelinated fiber bundle that connects Broca's and Wernicke's areas, has been frequently studied.[12,23] However, results have been inconsistent, with reports of both higher[19,20,24] and lower[18,25,26] fractional anisotropy (FA) in patients with AH. Studies have also reported lower FA in SCZ with verbal AH compared to controls within the left inferior fronto-occipital fasciculus (IFO), the left uncinate fasciculus (UF), and the right superior longitudinal fasciculus (SLF), as well as within interhemispheric auditory pathways.[18,27–29] Since most studies have focused on a selection of fiber tracts, the full extent of the relationship between AH in SCZ and WM microstructure remains unclear.

Numerous studies have employed current measures of AH, ie, measures of AH spanning a specified time before clinical inclusion to the study (typically 1–2 weeks). Interestingly, a recent study identified 3 distinct courses of AH during the first 10 years of illness in SCZ.[30] These were characterized by initially low and subsequently decreasing severity, high and fluctuating severity, and high and increasing severity. In clinically stable populations, current measures of AH will tend to identify the latter 2 groups as hallucinators, whereas lifetime measures do not distinguish between the groups. As such, current and lifetime measures are sensitive to different state- and trait-related components. Current measures of AH may be better suited for identifying participants with frequent and persistent hallucinations. This group has been hypothesized to exhibit specific WM microstructure alterations.[31] However, lifetime measures of AH may provide complementary information about susceptibility toward AH.

Leveraging the shared variation across DTI metrics and fiber tracts can provide information beyond analyzing each metric and fiber tract in isolation.[32–34] For example, Chamberland et al[35] identified principal components that explained 80% of the variation across fiber tracts and diffusion measures. Their results revealed age-related effects, some of which were not detectable at the level of individual DTI metrics. Importantly, the components loaded onto diffusion measures with shared sensitivities to specific tissue properties, demonstrating that this approach yields biologically interpretable information. Using a similar approach, Vaher et al[34] found evidence for both generalized and tract-specific dysmaturation in preterm individuals. Thus, combining DTI metrics can enhance sensitivity to group differences and brain-behavior associations.[36–38]

Here, we investigated the relationship between current AH (ie, within a week of clinical inclusion) and FA, mean diffusivity (MD), radial diffusivity (RD), and axial diffusivity (AD) in patients with SCZ and healthy controls. We included a broad range of fiber tracts and DTI metrics and pooled variation across both fiber tracts and DTI metrics using an established dimensionality reduction framework.[33–35] We hypothesized lower FA and higher MD and RD in fiber tracts within the LAPC in patients with current AH.[4,18,21] Since patients without current AH may have a lifetime history of AH, we further subdivided this group into participants with and without a lifetime history of AH and contrasted them with healthy controls. We assessed the effects of psychotic symptom severity, age at onset, duration of illness, and antipsychotic medication use and dose in exploratory analyses. Finally, we examined if putative group differences were influenced by sex, age, head size, or BMI.

Methods

Participants

Participants diagnosed with SCZ and age-and-sex-matched healthy controls were included from the ongoing Thematically Organized Psychosis (TOP; $n = 659$) study at the Oslo University Hospital, Norway, and from the Human Brain Informatics (HUBIN; $n = 92$) project at Karolinska Institutet in Stockholm, Sweden. Patients were referred from psychiatric units and outpatient clinics in the greater Oslo region and from catchment areas within the North-Western Stockholm County, respectively. Healthy controls were recruited based on population registries for both TOP and HUBIN and among hospital staff for HUBIN.

Exclusion criteria included an age outside the range 18–65 years, intelligence quotient (IQ) less than 70, and neurologic illness or previous moderate to severe head injury. Controls were also excluded if they had a history of substance abuse/dependency or a first-degree relative diagnosed with a severe psychiatric disorder as determined by a screening interview and, for TOP, the Primary Care Evaluation for Mental Disorders (Prime-MD).[39]

Healthy controls were age-and-sex-matched to the patient group using genetic matching without replacement in the *MatchIt* package[40] in R. We used the model Diagnosis ~ Age + Sex + Scanner with exact matching on MRI scanner. This approach avoids issues with propensity score matching, which may not ensure close pairings of participants.[41]

The final study sample ($n = 280$) included 140 age- and sex-matched healthy controls (mean age: 33.2; range = [18.4, 63.6]; 35.7% female) and 140 patients with SCZ (mean age: 33.3; range = [18.5, 63.6]; 35.7% female) diagnosed with schizophrenia ($n = 106$), schizophreniform disorder ($n = 24$), and schizoaffective disorder ($n = 10$).

Clinical Assessment

For patients in TOP, diagnoses and lifetime symptoms were assessed using the Structured Clinical Interview for DSM-IV axis 1 disorders (SCID-IV),[42] and current symptoms, ie, the week before clinical assessment, were evaluated with the Positive and Negative Syndrome Scale, PANSS.[43] PANSS scores were converted to symptom factors from the Wallwork 5-factor model,[44] ie, positive (P1 + P3 + P5 + G9), negative (N1 + N2 + N3 + N4 + N6 + G7), disorganized (P2 + N5 + G11), excited (P4 + P7 + G8 + G14), and depressive (G2 + G3 + G6) symptom factors. For patients in HUBIN, diagnoses and lifetime symptoms were assessed using the SCID-III-R[42] and Schedules for Clinical Assessment in Neuropsychiatry (SCAN),[45] and current symptoms were evaluated with the Scales for the Assessment of Positive and Negative Symptoms, SAPS and SANS.[46,47]

Antipsychotic medication use was determined via interviews. To compare doses across antipsychotic medication type and dosage, we converted antipsychotic medication dosage to chlorpromazine equivalent doses (CPZ; mg/day).[48] We defined age at onset as age at first psychotic episode (verified by SCID-IV, SCID-III-R, or SCAN) and duration of illness as years from age at onset to age at MRI scan. IQ was assessed with the Wechsler Abbreviated Scale of Intelligence (WASI-II) in TOP and the Wechsler Adult Intelligence Scale (WAIS) in HUBIN. Alcohol and drug use was assessed with the Alcohol Use Disorder Identification Test (AUDIT)[49] and the Drug Use Disorders Identification Test (DUDIT).[50] Psychosocial functioning was rated using the split version of the Global Assessment of Functioning Scale (GAF).[51]

We determined current AH status based on the PANSS-P3 item in TOP and the SAPS-H1 item in HUBIN. For TOP, we defined the current AH group (AH+) as participants with a P3 score ≥3, and conversely the current non-AH group (AH−) as those with a P3 score <3. For HUBIN, we defined the current AH group as having an H1 score ≥2, and the current non-AH group (AH−) as H1 <2. For the follow-up analyses including a lifetime history of AH, we further subdivided the AH− group into 2 subgroups: Patients with a lifetime history of AH (L-AH) and patients who had never experienced AH (N-AH). To determine the lifetime history of AH, we used the SCID-B16 item for TOP and the 17.004 item in SCAN for HUBIN.

The AH+ group (n = 59) comprised 49 patients with schizophrenia (83.1%) and 10 patients with schizoaffective disorder (16.9%), and the AH− group (n = 81) comprised 57 patients with schizophrenia (70.4%), 14 patients with schizoaffective disorder (17.3%), and 10 patients with schizophreniform disorder (12.3%). The L-AH group comprised 49 patients and the N-AH group comprised 24 patients. Eight patients with missing data on lifetime AH were excluded from the latter stratification. See supplementary note 1 for additional information on the clinical assessment of AH.

MRI Acquisition and Processing

MRI data was acquired on 3 different 3T scanner platforms; a GE Signa HDxt and a GE Discovery MR750 at Oslo University Hospital (OUS), Ullevål, Oslo, and a GE Discovery MR750 at Karolinska Institutet in Stockholm, Sweden. See supplementary table 3 for acquisition parameters. DTI images were processed using an optimized pipeline[52] and FSL[53] (version 6.0.3) with corrections for noise,[54] Gibbs ringing,[55] echo-planar imaging (EPI) motion, eddy currents, and susceptibility distortions. DTI metrics were estimated with *dtifit* using the linear weighted least squares algorithm.

Fiber tractography was performed with XTRACT[56] in FSL using well-validated and robust protocols for automated fiber tractography. Median FA, MD, RD, and AD were extracted for 39 inter- and intra-hemispheric fiber tracts. See figure 1 and table 1 for overviews of the included fiber tracts and supplementary note 2 for information on fiber tract selection. To compute intracranial volume (ICV), we used Sequence Adaptive Multimodal Segmentation (SAMSEG)[57] with default parameters using a single T1-weighted image as input.

The batch-adjustment algorithm ComBat[58] was used to adjust for non-biological variation in DTI metrics due to differences in pulse sequence and scanner platform. This is a Bayesian adjustment method originally developed for removing batch effects in genomics that has since been applied to a wide range of neuroimaging data, including DTI.[59] Age, sex, and diagnosis were entered as variables of interest. See supplementary figure 1 for boxplots showing the effect of scanner harmonization and supplementary note 3 for information on quality assurance procedures.

Statistical Analyses

Statistical analyses were performed in R (version 4.2.3; R Core Team, 2018). All regression models included age, age^2, and sex as covariates, where we included age^2 since the relationship between age and DTI metrics may be nonlinear.[60] Cohen's d effect sizes (d) were obtained from t-values using the *effectsize* package[61] implemented in R. We adjusted P-values for the false discovery rate (FDR) using the Benjamini–Hochberg procedure.[62] An FDR-adjusted P-value of <0.05 was considered statistically significant.

Demographic and Clinical Group Comparisons. We assessed group differences in age, sex, years of education, handedness, BMI, IQ, AUDIT and DUDIT scores, age at onset, duration of illness, number of psychiatric hospital admissions, GAF functioning (GAF-F) and symptom

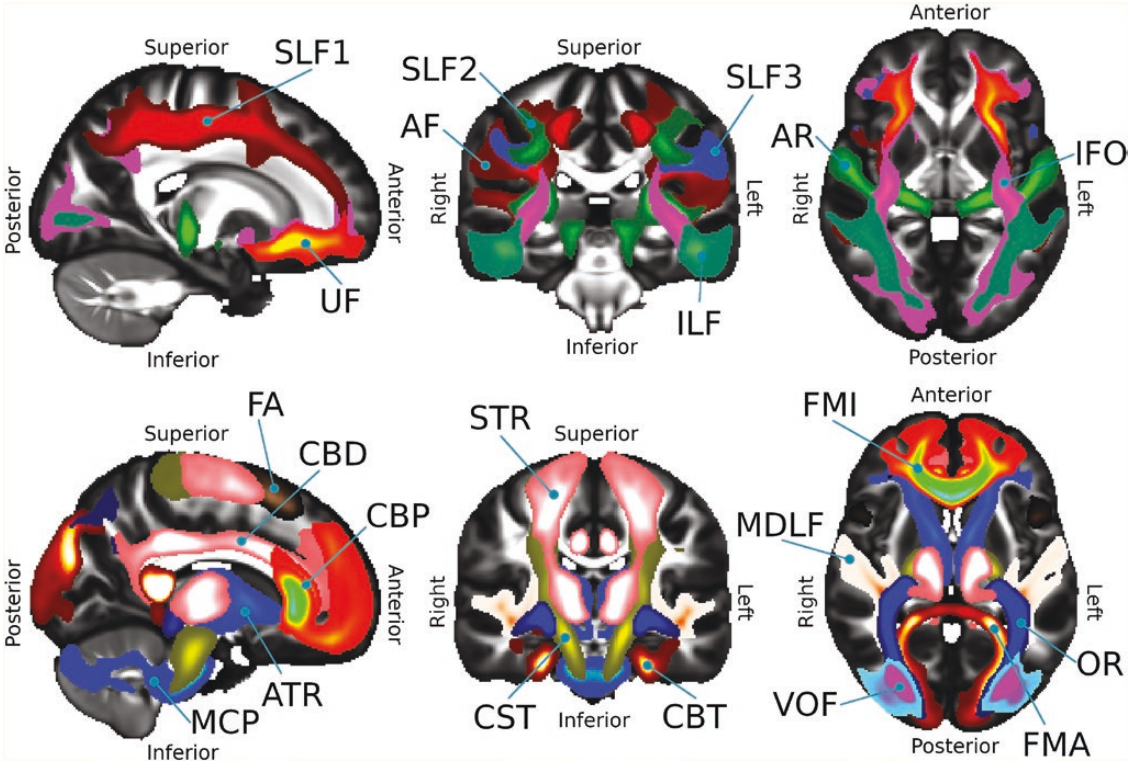

Fig. 1. Visualization of the fiber tracts included in the present study. The top row shows fiber tracts within the language and auditory processing circuitry (LAPC). The bottom row shows the other fiber tracts.

(GAF-S) scores, the 5 Wallwork symptom factors, antipsychotic use (yes/no), CPZ-equivalent doses, and antiepileptic and antidepressant use. Continuous and categorical variables were compared using the Kruskal-Wallis test and the χ^2 test, respectively.

Tract- and Metric-Specific Analyses. To assess group differences in tract-specific DTI metrics in AH+ and AH− compared to healthy controls, we fitted univariate regression models with DTI metrics (FA, MD, RD, or AD) in each of the 39 fiber tracts as dependent variables and current AH status as the variable of interest. To assess tract-wise group differences between AH+ and AH− for each DTI metric, we fitted similar models among AH+ and AH− only.

In follow-up analyses, we explored group differences in tract-specific DTI metrics in 2 subgroups of patients without current hallucinations. In these analyses, we compared patients who did not have current hallucinations but did (L-AH) or did not (N-AH) have a lifetime history of AH with healthy controls and, among patients only, each other. The aim of these analyses was to assess whether any differences between AH− and CTR were driven by lifetime AH.

Finally, we compared tract-specific DTI metrics in all patients with SCZ, ie, current AH+ and AH− combined, with those of controls in regression models where diagnostic group was included as the variable of interest.

Uni- and Multimodal General Factor Analyses. To assess the patterns of associations with AH status across WM fiber tracts and DTI metrics, we extracted uni- and multimodal general factors (g-factors) following a previously established dimensionality reduction framework.[33–35] This entailed principal component analysis (PCA) across fiber tracts for each DTI metric to create unimodal g-factors and across both fiber tracts and DTI metrics to create multimodal g-factors. The PCA was performed in the complete dataset (ie, 280 participants). PCA was conducted by singular value decomposition on scaled tract-specific DTI metrics using the *prcomp* function in R. To assess the suitability of the data for factor analysis, we used the Kaiser–Meyer–Olkin test[63] and Bartlett's test of sphericity, which measure the amount of shared variance and the overall degree of correlation within the variables.

Unimodal g-factors were created by conducting PCA on all 39 fiber tracts, for each DTI metric separately. Based on the literature,[33–35] we aimed to identify 1 general factor for each DTI metric to capture shared variation across fiber tracts. We therefore extracted the first principal components. This yielded 4 g-factors, g-FA, g-MD, g-RD, and g-AD, quantifying the proportion of shared variation across fiber tracts for each DTI metric.

Multimodal g-factors were created by conducting PCA on all tracts and DTI metrics simultaneously. That is, we performed PCA on a matrix with rows corresponding to subject-tract pairs (ie, 39 rows per subject) and 4 columns

Table 1. List of fiber tracts of interest.

	Abbreviation	Full name
Language and auditory processing circuitry (LAPC)	AF	Arcuate Fasciculus
	AR	Acoustic Radiation
	ILF	Inferior Longitudinal Fasciculus
	IFO	Inferior Fronto-Occipital Fasciculus
	SLF1	Superior Longitudinal Fasciculus 1
	SLF2	Superior Longitudinal Fasciculus 2
	SLF3	Superior Longitudinal Fasciculus 3
	UF	Uncinate Fasciculus
Association fibers	FA	Frontal Aslant
	MDLF	Middle Longitudinal Fasciculus
	VOF	Vertical Occipital Fasciculus
Limbic fibers	CBD	Cingulum subsection: Dorsal
	CBP	Cingulum subsection: Peri-genual
	CBT	Cingulum subsection: Temporal
Commissural fibers	FMA	Forceps Major
	FMI	Forceps Minor
	MCP	Middle Cerebellar Peduncle
Projection fibers	ATR	Anterior Thalamic Radiation
	CST	Corticospinal Tract
	OR	Optic Radiation
	STR	Superior Thalamic Radiation

corresponding to FA, MD, RD, and AD measurements. Prior studies found that 2 components were required to capture multimodal variation.[33–35] We therefore extracted the first and second principal components, resulting in 2 multimodal g-factors, g-Dim1 and g-Dim2, quantifying the proportion of shared variation across both DTI metrics and fiber tracts.

To compare uni- and multi-modal g-factors in AH+ and AH− with those of healthy controls, we fitted separate regression models with current AH (AH+/AH−) as the variable of interest and each g-factor as dependent variables. We fitted similar models among patients to directly compare g-factors of AH+ with those of AH−.

Associations With Clinical and Demographic Variables. We performed additional analyses to investigate if clinical characteristics other than AH status were associated with DTI measurements. Among patients we assessed relationships between uni- and multimodal g-factors and the following clinical variables: Age at onset, duration of illness, antipsychotic medication use (yes/no), CPZ-equivalent dose, and the 5 Wallwork symptom factors (positive, negative, depressed, disorganized, and excited). In these analyses, we fitted separate univariate regression models for each clinical measure as variables of interest and each g-factor as dependent variables.

Since ICV and BMI can contribute to variation in DTI metrics,[64] we next examined if group differences in g-factors were confounded by these variables. To do this, we fitted separate regression models with ICV and BMI included as independent variables together with the current AH term. We fitted the models both in the whole sample, for the contrast of AH+ and AH− with controls, and among patients only, for the direct comparison of AH+ with AH−.

Finally, we examined if group differences in current AH differed by age or sex. To do this, we fitted regression models including interaction terms for current AH by age and age^2 and sex, as well as their respective main effects. Uni- and multimodal g-factors were specified as dependent variables and separate models were fitted for each putative interaction.

Results

Demographic and Clinical Group Comparisons

Years of education and IQ were lower in patients, AH+, and AH− compared to controls. DUDIT scores were higher in patients, AH+, and AH− compared to controls. GAF-F and GAF-S scores were lower in AH+ compared to AH−. Positive, excited, and depressed symptom factors, and CPZ-equivalent doses were higher in AH+ compared to AH−. See table 2 for clinical and demographic variables for the final sample and supplementary tables 1 and 2 for the same divided by dataset.

Tract- and Metric-Specific Analyses

See figure 2 for bar plots of Cohen's *d* effect sizes for MD and RD, supplementary figure 7 for bar plots of Cohen's *d* effect sizes for FA and AD, and supplementary tables 4–7 for Cohen's *d* effect sizes and FDR-adjusted and unadjusted *P*-values for each DTI metric.

We observed no significant group differences between AH+ and AH− and healthy controls for FA or AD. Compared to controls, AH− had higher MD in several

Table 2. Demographic and clinical characteristics by group.

	CTR (N = 140)	SCZ (N = 140)	Test of difference (SCZ vs CTR)	AH+ (N = 59)	AH− (N = 81)	Test of difference (AH+ vs AH−)
Demographics and IQ						
Age [years]	33.2 (11.9)	33.3 (12.0)	N.S.	34.0 (12.1)	32.8 (11.9)	N.S.
Sex [female]	50 (35.7%)	50 (35.7%)	N.S.	20 (33.9%)	30 (37.0%)	N.S.
Education [years]	14.2 (2.4)	12.3 (2.3)	H = 42.3, P < 1E-10 SCZ < CTR	12.2 (2.6)	12.3 (2.0)	N.S.
Handedness [right]	69 (87.3%)	70 (90.9%)	N.S.	33 (89.2%)	37 (92.5%)	N.S.
BMI	24.6 (3.6)	25.9 (5.3)	N.S.	25.2 (4.9)	26.4 (5.6)	N.S.
IQ[a]	113.4 (10.4)	101.8 (13.3)	H = 45.3, P < 1E-10 SCZ < CTR	101.8 (13.6)	101.8 (13.2)	N.S.
Alcohol and drug use						
AUDIT	5.7 (3.2)	6.7 (6.3)	N.S.	7.7 (7.5)	6.1 (5.3)	N.S.
DUDIT	0.3 (1.3)	5.1 (8.1)	H = 37.7, P < 1E-9 SCZ > CTR	6.4 (9.1)	4.3 (7.3)	N.S.
Clinical variables						
Age at onset [years]	N.A.	22.2 (6.3)	N.A.	21.1 (5.1)	22.9 (7.1)	N.S.
Duration of illness [years]	N.A.	10.6 (10.5)	N.A.	12.8 (11.4)	8.9 (9.5)	N.S.
Psychiatric hospital admissions[a]	N.A.	2.9 (3.3)	N.A.	3.1 (3.3)	2.8 (3.3)	N.S.
GAF-F	N.A.	47.3 (12.1)	N.A.	42.9 (9.9)	50.5 (12.5)	H = 11.0, P < .001 AH+ < AH−
GAF-S	N.A.	47.6 (12.5)	N.A.	41.7 (8.2)	51.9 (13.3)	H = 25.3, P < 1E-6 AH+ < AH−
PANSS factors[a]						
Positive[a]	N.A.	9.0 (4.0)	N.A.	12.4 (2.5)	6.8 (3.1)	H = 55.9, P < 1E-13 AH+ > AH−
Negative[a]	N.A.	13.2 (5.1)	N.A.	14.0 (5.6)	12.7 (4.8)	N.S.
Disorganized[a]	N.A.	5.6 (2.9)	N.A.	6.2 (3.5)	5.3 (2.3)	N.S.
Excited[a]	N.A.	5.3 (2.1)	N.A.	6.0 (2.9)	4.9 (1.1)	H = 3.9, P < .05 AH+ > AH−
Depressed[a]	N.A.	7.8 (2.9)	N.A.	8.7 (2.6)	7.3 (2.9)	H = 7.2, P < .01 AH+ > AH−
Medication use						
AP use [yes]	N.A.	129 (92.8%)	N.A.	52 (89.7%)	77 (95.1%)	N.S.
CPZ-equiv. AP dose [mg/day]	N.A.	347.7 (206.6)	N.A.	428.9 (256.9)	290.3 (137.0)	H = 8.8, P < .01 AH+ > AH−
Antiepileptic use[a] [yes]	N.A.	14 (12.6%)	N.A.	4 (9.5%)	10 (14.5%)	N.S.
Antidepressant use[a] [yes]	N.A.	29 (26.1%)	N.A.	13 (31.0%)	16 (23.2%)	N.S.

Note: H, Kruskal–Wallis test statistic; AUDIT, Alcohol Use Disorders Identification Test; DUDIT, Drug Use Disorders Identification Test; GAF-F, Global Assessment of Functioning (GAF) functioning scale; GAF-S, GAF symptom scale; PANSS, Positive and Negative Syndrome Scale; AP, antipsychotic medication; CPZ-equiv., chlorpromazine-equivalent; N.A., not applicable; N.S., not significant.
[a]TOP dataset only.

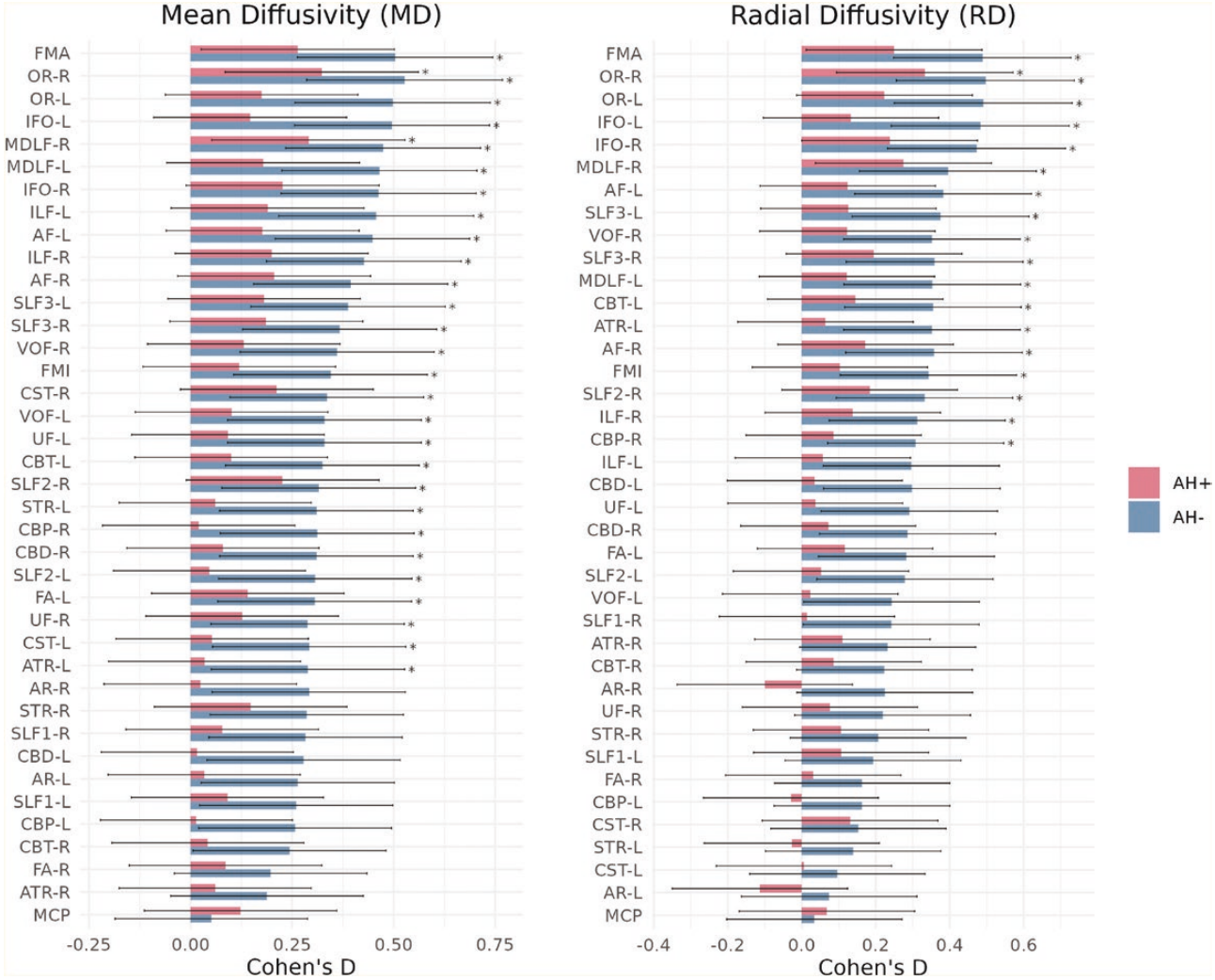

Fig. 2. Cohen's *d* effect sizes for the contrast between patients with schizophrenia with (AH+) and without (AH−) current hallucinations and healthy controls for radial diffusivity (RD) and mean diffusivity (MD). Fiber tracts are ordered by estimated effect size. Error bars indicate 95% confidence intervals. Significant differences after FDR correction are marked with asterisks.

fiber tracts, including the bilateral AF, right AR, left ATR, right CBD, right CBP, left CBT, bilateral CST, left FA, bilateral ILF, bilateral IFO, bilateral MDLF, bilateral OR, bilateral STR, right SLF1, bilateral SLF2, bilateral SLF3, bilateral UF, bilateral VOF, FMA, and FMI. We also observed higher MD in AH+ in the right MDLF and the right OR compared to controls.

Higher RD was observed in AH− for the bilateral AF, left ATR, right CBP, left CBT, right ILF, bilateral IFO, bilateral MDLF, bilateral OR, right SLF2, bilateral SLF3, right VOF, FMA, and FMI compared to controls. We also observed higher RD in the right OR in AH+ compared to controls. There were no significant differences between AH+ and AH− after correction for multiple testing for any of the DTI metrics.

We found no group differences between either L-AH or N-AH and healthy controls for FA and AD. Compared to controls, L-AH had higher MD in the left AF, left ILF, bilateral IFO, bilateral MDLF, bilateral OR, and the FMA. We also observed higher RD in the bilateral IFO, OR and the FMA in L-AH compared to controls. Only the right ILF showed higher MD in N-AH compared to controls. In the direct comparison between L-AH and N-AH, the only significant difference was for FA in the right FA tract indicating lower FA in N-AH compared to L-AH.

When comparing the whole patient group (SCZ) with controls, significant differences were found in a wide range of fiber tracts for MD, RD, and AD, but not FA. See supplementary figures 8 and 9 for bar plots of Cohen's *d* effect sizes, supplementary tables 8–11 for Cohen's *d* effect sizes and FDR-adjusted and unadjusted p-values for each DTI metric, and supplementary note 4 for a description of these results.

Uni- and Multimodal General Factor Analyses

Kaiser–Meyer–Olkin test and Bartlett's test of sphericity indicated excellent suitability for factor analysis. See

supplementary figures 10–13 for correlation matrices between fiber tracts and supplementary figure 14 for a density plot of the correlations.

Explained variance of the unimodal g-factors ranged from 41.1% for g-FA to 63.9% for g-MD, whereas the second principal components only explained between 5.4% for RD to 6.6% for AD. See supplementary figure 15 for scree and variable contribution plots and supplementary table 12 for tract-wise correlations with each general factor.

For the multimodal g-factors, the explained variance was 64.3% for g-Dim1 and 32.5% for g-Dim2. Correlations with g-Dim1 were negative ($r = -0.72$) for FA, and positive for MD ($r = 0.95$), RD ($r = 0.99$), and AD ($r = 0.42$). For g-Dim2 the correlations were negative for FA ($r = -0.66$), MD ($r = -0.25$), and AD ($r = 0.88$), and positive for RD ($r = 0.13$). Most of the variance of g-Dim1 was contributed by RD (37.8%), MD (35.3%), and FA (19.9%). For g-Dim2, AD (60.1%) and FA (33.9%) contributed the most to the variance. See supplementary table 13 for correlations and contributions of each DTI metric to the multimodal g-factors and supplementary figure 16 for scree plots and variable contribution plots.

In the regression analyses we found significant group differences between AH− and controls for all uni- and multimodal g-factors, except g-FA. These associations indicated lower g-Dim2 and higher g-MD, g-RD, and g-AD in AH− compared to controls. No significant differences between AH+ and controls were observed for any of the g-factors. See figure 3 for violin plots of each g-factor for each group adjusted for age, age^2, and sex.

Associations With Clinical and Demographic Variables

We found no significant associations between uni- and multimodal g-factors and age at onset, duration of illness, antipsychotic medication use (yes/no), CPZ-equivalent dose, or the positive, negative, disorganized, depressed, or excited Wallwork symptom factors.

ICV was significantly associated with g-FA, g-RD, g-AD, and g-Dim2. Group differences between AH− and healthy controls remained significant for g-RD, g-AD, g-Dim2 when also adjusting for ICV. There were no significant associations between g-factors and BMI or significant interactions between current AH status and age or sex for any of the g-factors.

Discussion

The main finding of the present study was a widespread pattern of tract-wise differences represented by higher MD and RD in patients with SCZ *without* current AH (AH−) compared to healthy controls. Surprisingly, only MD in the right middle longitudinal fasciculus (MDLF) and both MD and RD in the right optic radiation (OR) differed significantly in patients with current AH (AH+) relative to healthy controls, indicating higher MD and RD. In line with these findings, uni- and multimodal g-factors differed only between the AH− group and healthy controls. These findings suggest that altered DTI metrics in schizophrenia are not a specific feature underlying AH and instead point toward a more complex relationship between WM microstructure and AH.

Most previous DTI studies on AH in SCZ have focused on a limited set of fiber tracts under the assumption that WM alterations relevant to AH are localized within the language and auditory processing circuitry (LAPC). We observed higher MD and RD in several fiber tracts within the LAPC in patients without current AH compared to controls. These fiber tracts included the arcuate fasciculus (AF), inferior longitudinal fasciculus (ILF), the superior longitudinal fasciculus (SLF), inferior fronto-occipital fasciculus (IFO), and the uncinate fasciculus (UF). We also found associations with AH in interhemispheric fiber tracts including the forceps major and minor (FMA and FMI) and the dorsal, peri-genual and temporal subsections of the cingulum bundle (CBD, CBP, and CBT), as well as in fiber tracts not in the LAPC, eg, the vertical occipital fasciculus (VOF) and the OR. The involvement of interhemispheric pathways in AH in SCZ has been proposed previously, but findings have been inconsistent.[4,18,27,29,65] Our results provide evidence for the involvement of interhemispheric fiber tracts in AH and suggest that the relationship between WM microstructure and AH is widespread rather than confined to the LAPC.

The AH− group differed significantly compared to healthy controls for all uni- and multimodal g-factors, except g-FA, suggesting a generalized effect. In agreement with the literature,[33–35] the first principal components explained most of the variation in the unimodal principal component analyses (41.1%–63.9%), while the second principal components explained only 5.4%–6.6%. For the multimodal g-factors, the second principal component explained a non-negligible proportion of the variation, which is also in line with past studies.[33–35] Interestingly, g-AD was significantly higher in AH− patients compared to controls although there were no significant tract-specific differences for AD. Similarly, g-Dim2, which mostly received contributions from FA (33.9%) and AD (60.1%), was significantly lower in AH− compared to controls. These findings may indicate enhanced sensitivity to WM microstructure differences with the use of dimensionality reduction.

In a study on individuals at clinical high risk for psychosis and patients with first-episode psychosis, Sato et al[21] found positive associations between current hallucination severity and MD in the left SLF and inferior IFO. Though this contrasts with our findings, the patients included in our study had a relatively long duration of illness (mean = 10.6 years). Similarly, Salisbury et al[14] reported associations between current hallucination

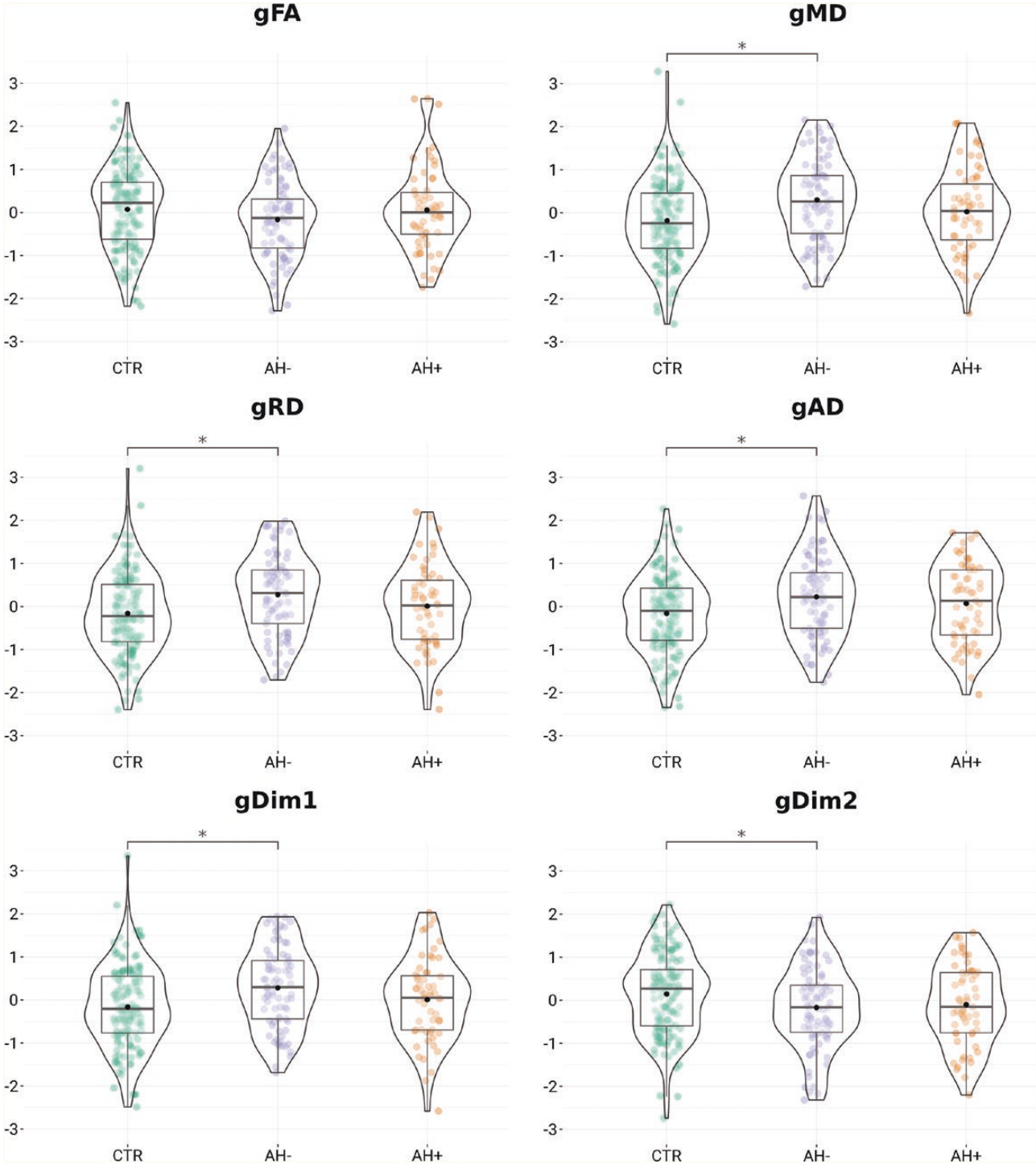

Fig. 3. Uni- and multimodal g-factors residualized with respect to age, age^2, and sex for controls (CTR), patients with current hallucinations (AH+), and patients without current hallucinations (AH−).

severity and quantitative anisotropy in first-episode psychosis.[66] Given the dynamic nature of WM microstructure,[60] it would be necessary to perform longitudinal data collection to assess trajectories of WM microstructure and AH. We could not ascertain if the observed group differences emerged after illness onset or point toward a subgroup of patients that are less prone to AH and more likely to exhibit WM differences as measured with DTI. Notably, our follow-up analyses on patients without current AH but with a lifetime history of AH (L-AH) showed group differences between patients with lifetime AH compared to controls in several fiber tracts. On the other hand, patients with no lifetime history of AH (N-AH) did not differ compared to healthy controls. Given the

small number of participants with no lifetime history of AH ($n = 24$), this may reflect a loss of power in these analyses. We encourage future studies to assess the longitudinal course of WM microstructure and relationships with AH as the illness progresses from an acute to a more chronic phase.

There were no significant group differences in g-factors between patients who used antipsychotic medication compared to patients who did not, nor significant associations between g-factors and CPZ-equivalent dose. However, only a small number of patients did not use antipsychotic medication and we did not have data on cumulative exposure which may have challenged our ability to detect medication-related effects. The literature on the effects of antipsychotic medication on DTI metrics is sparse and has largely focused on FA.[67] Previous studies have reported both reduced[68] and increased[69–71] FA following antipsychotic treatment. Further studies with more comprehensive medication data are needed to characterize the effects of antipsychotic medication on WM microstructure.

It should be noted that although associations with DTI metrics are often ascribed to microstructural tissue properties such as degree of myelination, fiber tract organization, axonal ordering and density, and membrane permeability, the specificity is low and DTI metrics reflect a combination of neurobiological processes.[72,73] In particular, the interpretation of FA as a measure of white matter integrity has been questioned.[74] While it is not possible to directly link DTI metric alterations to microstructure, DTI metrics exhibit different sensitivities to distinct tissue properties. For instance, joint diffusion and histological studies in the cuprizone model of demyelination in mice indicate that RD is related to de- and re-myelination,[75–77] whereas AD may be more sensitive to axonal damage.[78] Similarly, MD has been reported to be more sensitive to myelin-staining indices than either FA or RD.[79] We therefore recommend that future studies employ a wider range of diffusion metrics to investigate putative WM microstructural correlates of AH in SCZ.

The present study highlights some important challenges when mapping symptoms onto functionally defined brain networks, that are also relevant in the context of other symptom constructs such as Formal Thought Disorder (FTD).[80] Importantly, longitudinal assessments of both symptoms and brain structure are needed to investigate the time-varying course of AH, its relationship with illness duration and phase, and to track putative compensatory changes reflecting WM plasticity. The challenge of clinical heterogeneity and overlap with variation in healthy controls may be partly mitigated by employing a symptom capture approach to assess within-subject neural correlates of AH.[31] Furthermore, experimental paradigms hold great potential for formulating and testing mechanistic models of AH and recent animal studies on experimentally induced hallucination-like percepts have yielded insights difficult to achieve in studies on humans.[81] Finally, most studies on AH do not distinguish between distinct features of AH such as frequency, localization of the percepts, and the valence of voices, which may reflect discrete neurobiological mechanisms and future studies should strive toward a more detailed characterization of the phenomenology of AH.

Strengths of the study included a clinically well-characterized patient group, which allowed us to test associations with current antipsychotic medication use and dose, duration of illness, and psychotic symptoms. Importantly, our relatively large sample size afforded us the statistical power to assess a broader range of fiber tracts than previous studies and to combine and compare FA, MD, RD, and AD through dimensionality reduction. Fiber tractography was performed using a reproducible framework at the subject-level rather than relying on maps from subject space to a common template. This improves the accuracy of fiber tract reconstruction by taking individual anatomical differences into account.

Several important limitations should be considered when evaluating the results of this study. Since the data were cross-sectional, we could not estimate longitudinal changes to WM microstructure. Similarly, fluctuations in the presence and severity of AH may have impacted the stratification approach. We also did not have access to cumulative exposure to antipsychotic medication or duration of AH. The current AH+ group was smaller than the current AH− group which may have reduced sensitivity. In line with some previous studies,[65,82–84] we only observed significant differences compared to controls and not between AH+ and AH−. As such, strong conclusions on the differences between AH+ and AH− should be avoided. Hallucination status was assessed with 2 different instruments, PANSS and SAPS, in the TOP and the HUBIN datasets, and there were differences in the clinical characteristics, with the patients in the HUBIN dataset having a longer duration of illness. Furthermore, while we matched patients and controls on scanner and corrected for scanner effects using a well-established harmonization procedure, we cannot rule out that residual effects of scanner remained. Finally, DTI metrics are indirect measures of WM microstructure and strong biophysical conclusions should be avoided.[74,85]

In conclusion, we found higher MD and RD across widespread fiber tracts mainly in patients without current AH compared to controls. In contrast to our hypothesis, patients with SCZ and current AH only differed significantly relative to healthy controls for MD in the MDLF and for MD and RD in the OR. These results challenge the idea that altered DTI metrics in the LAPC in patients with SCZ is a specific feature underlying AH. Instead, the findings suggest a more complex relationship between AH status and WM microstructure. We encourage future studies to investigate the longitudinal

course of AH and WM microstructure and to employ more direct measures of myelin alongside detailed clinical evaluations of AH.

Supplementary Material

Supplementary data are available at *Schizophrenia Bulletin Open* online.

Acknowledgments

We are grateful to the study participants who were willing to participate in this project and the clinicians who were involved in recruitment and assessments at NORMENT and as part of the HUBIN project. Data services were provided by the Services for Sensitive Data (TSD) facilities, operated and developed by the TSD service group in the University of Oslo IT services department (USIT). O.A.A. has received speaker's honoraria from Lundbeck and Sunovion and is a consultant for HealthLytix. I.A. has received a speaker's honorarium from Lundbeck. The authors report no conflicts of interest.

Funding

The work was supported by The Research Council of Norway (grant numbers 223273, and 274359), the K. G. Jebsen Foundation (grant number SKGJ-MED-008), Helse Sør-Øst RHF (grant numbers 2017-097, 2019-104, and 2020-020), the Swedish Research Council (K2012-61X-15078-09-3, K2015-62X-15077-12-3, and 2017-00949), the European Research Council under the European Union Horizon 2020 research and innovation program (grant number 802998), the regional agreement on medical training and clinical research between Stockholm County Council and the Karolinska Institutet, the Knut and Alice Wallenberg Foundation, and the HUBIN project.

Ethical declaration

The studies were carried out in accordance with the Helsinki Declaration and all participants provided written informed consent. The TOP project was approved by the Regional Committee for Medical Research Ethics and the Norwegian Data Inspectorate. The HUBIN project was approved by the Swedish Ethical Review Authority at Karolinska Institutet. Data handling complied with Norwegian Data Protection Authority and GDPR regulations.

References

1. Waters F, Collerton D, Ffytche DH, *et al.* Visual hallucinations in the psychosis spectrum and comparative information from neurodegenerative disorders and eye disease. *Schizophr Bull.* 2014;40(Suppl 4):S233–S245. doi:10.1093/schbul/sbu036
2. Chiang YH, Beckstead JW, Lo SC, Yang CY. Association of auditory hallucination and anxiety symptoms with depressive symptoms in patients with schizophrenia: a three-month follow-up. *Arch Psychiatr Nurs.* 2018;32(4):585–590. doi:10.1016/j.apnu.2018.03.014
3. Choi A, Ballard C, Martyr A, Collins R, Morris RG, Clare L; IDEAL Programme Team. The impact of auditory hallucinations on "living well" with dementia: findings from the IDEAL programme. *Int J Geriatr Psychiatry.* 2021;36(9):1370–1377. doi:10.1002/gps.5533
4. Shao X, Liao Y, Gu L, Chen W, Tang J. The etiology of auditory hallucinations in schizophrenia: from multidimensional levels. *Front Neurosci.* 2021;15:755870. doi:10.3389/fnins.2021.755870
5. Shergill SS, Kanaan RA, Chitnis XA, *et al.* A diffusion tensor imaging study of fasciculi in schizophrenia. *Am J Psychiatry.* 2007;164(3):467–473. doi:10.1176/ajp.2007.164.3.467
6. Seok JH, Park HJ, Chun JW, *et al.* White matter abnormalities associated with auditory hallucinations in schizophrenia: a combined study of voxel-based analyses of diffusion tensor imaging and structural magnetic resonance imaging. *Psychiatry Res.* 2007;156(2):93–104. doi:10.1016/j.pscychresns.2007.02.002
7. Lee K, Yoshida T, Kubicki M, *et al.* Increased diffusivity in superior temporal gyrus in patients with schizophrenia: a diffusion tensor imaging study. *Schizophr Res.* 2009;108(1–3):33–40. doi:10.1016/j.schres.2008.11.024
8. Mørch-Johnsen L, Nesvåg R, Jørgensen KN, *et al.* Auditory cortex characteristics in schizophrenia: associations with auditory hallucinations. *Schizophr Bull.* 2017;43(1):75–83. doi:10.1093/schbul/sbw130
9. Neckelmann G, Specht K, Lund A, *et al.* MR morphometry analysis of grey matter volume reduction in schizophrenia: association with hallucinations. *Int J Neurosci.* 2006;116(1):9–23. doi:10.1080/00207450690962244
10. Kompus K, Westerhausen R, Hugdahl K. The "paradoxical" engagement of the primary auditory cortex in patients with auditory verbal hallucinations: a meta-analysis of functional neuroimaging studies. *Neuropsychologia.* 2011;49(12):3361–3369. doi:10.1016/j.neuropsychologia.2011.08.010
11. Hickok G. The cortical organization of speech processing: feedback control and predictive coding the context of a dual-stream model. *J Commun Disord.* 2012;45(6):393–402. doi:10.1016/j.jcomdis.2012.06.004
12. Friederici AD, Gierhan SM. The language network. *Curr Opin Neurobiol.* 2013;23(2):250–254. doi:10.1016/j.conb.2012.10.002
13. Fovet T, Yger P, Lopes R, *et al.* Decoding activity in Broca's area predicts the occurrence of auditory hallucinations across subjects. *Biol Psychiatry.* 2022;91(2):194–201. doi:10.1016/j.biopsych.2021.08.024
14. Salisbury DF, Wang Y, Yeh FC, Coffman BA. White matter microstructural abnormalities in the Broca's-Wernicke's-Putamen "Hoffman hallucination circuit" and auditory transcallosal fibers in first-episode psychosis with auditory hallucinations. *Schizophr Bull.* 2021;47(1):149–159. doi:10.1093/schbul/sbaa105
15. Feinberg I. Efference copy and corollary discharge: implications for thinking and its disorders. *Schizophr Bull.* 1978;4(4):636–640. doi:10.1093/schbul/4.4.636
16. Feinberg I, Guazzelli M. Schizophrenia – a disorder of the corollary discharge systems that integrate the motor systems of thought with the sensory systems of consciousness. *Br J Psychiatry.* 1999;174(3):196–204. doi:10.1192/bjp.174.3.196

17. Frith C. The neural basis of hallucinations and delusions. *CR Biol.* 2005;328(2):169–175. doi:10.1016/j.crvi.2004.10.012
18. Ćurčić-Blake B, Nanetti L, van der Meer L, *et al.* Not on speaking terms: hallucinations and structural network disconnectivity in schizophrenia. *Brain Struct Funct.* 2015;220(1):407–418. doi:10.1007/s00429-013-0663-y
19. Hubl D, Koenig T, Strik W, *et al.* Pathways that make voices: white matter changes in auditory hallucinations. *Arch Gen Psychiatry.* 2004;61(7):658–668. doi:10.1001/archpsyc.61.7.658
20. Psomiades M, Fonteneau C, Mondino M, *et al.* Integrity of the arcuate fasciculus in patients with schizophrenia with auditory verbal hallucinations: a DTI-tractography study. *NeuroImage Clin*. 2016;12:970–975. doi:10.1016/j.nicl.2016.04.013
21. Sato Y, Sakuma A, Ohmuro N, *et al.* Relationship between white matter microstructure and hallucination severity in the early stages of psychosis: a diffusion tensor imaging study. *Schizophr. Bull. Open.* 2021;2(1). doi:10.1093/schizbullopen/sgab015
22. Zhang X, Gao J, Zhu F, *et al.* Reduced white matter connectivity associated with auditory verbal hallucinations in first-episode and chronic schizophrenia: a diffusion tensor imaging study. *Psychiatry Res Neuroimaging*. 2018;273:63–70. doi:10.1016/j.pscychresns.2018.01.002
23. Wernicke C. *Der Aphasische Symptomencomplex: Eine Psychologische Studie Auf Anatomischer Basis*. Breslau: Max Cohn & Weigert; 1874.
24. Chawla N, Deep R, Khandelwal SK, Garg A. Reduced integrity of superior longitudinal fasciculus and arcuate fasciculus as a marker for auditory hallucinations in schizophrenia: a DTI tractography study. *Asian J Psychiatry.* 2019;44:179–186. doi:10.1016/j.ajp.2019.07.043
25. McCarthy-Jones S, Oestreich LKL, Whitford TJ; Australian Schizophrenia Research Bank. Reduced integrity of the left arcuate fasciculus is specifically associated with auditory verbal hallucinations in schizophrenia. *Schizophr Res.* 2015;162(1):1–6. doi:10.1016/j.schres.2014.12.041
26. Oestreich LKL, McCarthy-Jones S, Whitford TJ; Australian Schizophrenia Research Bank. Decreased integrity of the fronto-temporal fibers of the left inferior occipito-frontal fasciculus associated with auditory verbal hallucinations in schizophrenia. *Brain Imaging Behav*. 2016;10(2):445–454. doi:10.1007/s11682-015-9421-5
27. Wigand M, Kubicki M, von Hohenberg CC, *et al.* Auditory verbal hallucinations and the interhemispheric auditory pathway in chronic schizophrenia. *World J Biol Psychiatry.* 2015;16(1):31. doi:10.3109/15622975.2014.948063
28. Mulert C, Kirsch V, Whitford TJ, *et al.* Hearing voices: a role of interhemispheric auditory connectivity? *World J Biol Psychiatry* 2012;13(2):153–158. doi:10.3109/15622975.2011.570789
29. Knöchel C, Oertel-Knöchel V, Schönmeyer R, *et al.* Interhemispheric hypoconnectivity in schizophrenia: fiber integrity and volume differences of the corpus callosum in patients and unaffected relatives. *Neuroimage.* 2012;59(2):926–934. doi:10.1016/j.neuroimage.2011.07.088
30. Köhler-Forsberg O, Madsen T, Behrendt-Møller I, Nordentoft M. The 10-year trajectories of auditory hallucinations among 496 patients with a first schizophrenia-spectrum disorder: findings from the OPUS cohort. *Schizophr Res.* 2022;243:385–391. doi:10.1016/j.schres.2021.06.033
31. Whitford TJ, Ford JM, Mathalon DH, Kubicki M, Shenton ME. Schizophrenia, myelination, and delayed corollary discharges: a hypothesis. *Schizophr Bull.* 2012;38(3):486–494. doi:10.1093/schbul/sbq105
32. Cox SR, Ritchie SJ, Tucker-Drob EM, *et al.* Ageing and brain white matter structure in 3,513 UK Biobank participants. *Nat Commun.* 2016;7(1):13629. doi:10.1038/ncomms13629
33. Geeraert BL, Chamberland M, Lebel RM, Lebel C. Multimodal principal component analysis to identify major features of white matter structure and links to reading. *PLoS One.* 2020;15(8):e0233244. doi:10.1371/journal.pone.0233244
34. Vaher K, Galdi P, Blesa Cabez M, *et al.* General factors of white matter microstructure from DTI and NODDI in the developing brain. *Neuroimage.* 2022;254:119169. doi:10.1016/j.neuroimage.2022.119169
35. Chamberland M, Raven EP, Genc S, *et al.* Dimensionality reduction of diffusion MRI measures for improved tractometry of the human brain. *Neuroimage.* 2019;200:89–100. doi:10.1016/j.neuroimage.2019.06.020
36. Alnæs D, Kaufmann T, Doan NT, *et al.* Association of heritable cognitive ability and psychopathology with white matter properties in children and adolescents. *JAMA Psychiatry*. 2018;75(3):287–295. doi:10.1001/jamapsychiatry.2017.4277
37. Alnæs D, Kaufmann T, Marquand AF, Smith SM, Westlye LT. Patterns of sociocognitive stratification and perinatal risk in the child brain. *Proc Natl Acad Sci USA.* 2020;117(22):12419–12427. doi:10.1073/pnas.2001517117
38. Tønnesen S, Kaufmann T, de Lange AMG, *et al.* Brain age prediction reveals aberrant brain white matter in schizophrenia and bipolar disorder: a multisample diffusion tensor imaging study. *Biol Psychiatry Cogn Neurosci Neuroimaging*. 2020;5(12):1095–1103. doi:10.1016/j.bpsc.2020.06.014
39. Spitzer RL, Williams JB, Kroenke K, *et al.* Utility of a new procedure for diagnosing mental disorders in primary care. The PRIME-MD 1000 study. *JAMA.* 1994;272(22):1749–1756.
40. Ho D, Imai K, King G, Stuart EA. MatchIt: nonparametric preprocessing for parametric causal inference. *J Stat Softw*. 2011;42:1–28. doi:10.18637/jss.v042.i08
41. King G, Nielsen R. Why propensity scores should not be used for matching. *Polit Anal*. 2019;27(4):435–454. doi:10.1017/pan.2019.11
42. Spitzer RL, Williams JBW, Gibbon M, First MB. The structured clinical interview for DSM-III-R (SCID): I: history, rationale, and description. *Arch Gen Psychiatry.* 1992;49(8):624–629. doi:10.1001/archpsyc.1992.01820080032005
43. Kay SR, Fiszbein A, Opler LA. The Positive and Negative Syndrome Scale (PANSS) for schizophrenia. *Schizophr Bull.* 1987;13(2):261–276. doi:10.1093/schbul/13.2.261
44. Wallwork RS, Fortgang R, Hashimoto R, Weinberger DR, Dickinson D. Searching for a consensus five-factor model of the positive and negative syndrome scale for schizophrenia. *Schizophr Res.* 2012;137(1):246–250. doi:10.1016/j.schres.2012.01.031
45. Wing JK, Babor T, Brugha T, *et al.* SCAN: schedules for clinical assessment in neuropsychiatry. *Arch Gen Psychiatry.* 1990;47(6):589–593. doi:10.1001/archpsyc.1990.01810180089012
46. Andreasen NC. *Scale for the Assessment of Positive Symptoms (SAPS)*. Iowa City: University of Iowa.1984.
47. Andreasen NC. *Scale for the Assessment of Negative Symptoms (SANS)*. Iowa City: University of Iowa. 1983.
48. Jørgensen KN, Nesvåg R, Gunleiksrud S, Raballo A, Jönsson EG, Agartz I. First- and second-generation antipsychotic drug treatment and subcortical brain morphology

in schizophrenia. *Eur Arch Psychiatry Clin Neurosci.* 2016;266(5):451–460. doi:10.1007/s00406-015-0650-9

49. Saunders JB, Aasland OG, Babor TF, De La Fuente JR, Grant M. Development of the Alcohol Use Disorders Identification Test (AUDIT): WHO collaborative project on early detection of persons with harmful alcohol consumption-II. *Addiction.* 1993;88(6):791–804. doi:10.1111/j.1360-0443.1993.tb02093.x
50. Berman AH, Bergman H, Palmstierna T, Schlyter F. Evaluation of the Drug Use Disorders Identification Test (DUDIT) in criminal justice and detoxification settings and in a Swedish population sample. *Eur Addict Res.* 2005;11(1):22–31. doi:10.1159/000081413
51. Pedersen G, Hagtvet KA, Karterud S. Generalizability studies of the global assessment of functioning–split version. *Compr Psychiatry.* 2007;48(1):88–94. doi:10.1016/j.comppsych.2006.03.008
52. Maximov II, Alnæs D, Westlye LT. Towards an optimised processing pipeline for diffusion magnetic resonance imaging data: effects of artefact corrections on diffusion metrics and their age associations in UK Biobank. *Hum Brain Mapp.* 2019;40(14):4146–4162. doi:10.1002/hbm.24691
53. Jenkinson M, Beckmann CF, Behrens TEJ, Woolrich MW, Smith SM. FSL. *NeuroImage*. 2012;62(2):782–790. doi:10.1016/j.neuroimage.2011.09.015
54. Veraart J, Novikov DS, Christiaens D, Ades-aron B, Sijbers J, Fieremans E. Denoising of diffusion MRI using random matrix theory. *Neuroimage.* 2016;142:394–406. doi:10.1016/j.neuroimage.2016.08.016
55. Kellner E, Dhital B, Kiselev VG, Reisert M. Gibbs-ringing artifact removal based on local subvoxel-shifts. *Magn Reson Med.* 2016;76(5):1574–1581. doi:10.1002/mrm.26054
56. Warrington S, Bryant KL, Khrapitchev AA, *et al.* XTRACT—standardised protocols for automated tractography in the human and macaque brain. *Neuroimage.* 2020;217:116923. doi:10.1016/j.neuroimage.2020.116923
57. Puonti O, Iglesias JE, Van Leemput K. Fast and sequence-adaptive whole-brain segmentation using parametric Bayesian modeling. *Neuroimage.* 2016;143:235–249. doi:10.1016/j.neuroimage.2016.09.011
58. Johnson WE, Li C, Rabinovic A. Adjusting batch effects in microarray expression data using empirical Bayes methods. *Biostatistics*. 2007;8(1):118–127. doi:10.1093/biostatistics/kxj037
59. Fortin JP, Parker D, Tunç B, *et al.* Harmonization of multi-site diffusion tensor imaging data. *Neuroimage.* 2017;161:149–170. doi:10.1016/j.neuroimage.2017.08.047
60. Beck D, de Lange AMG, Maximov II, *et al.* White matter microstructure across the adult lifespan: a mixed longitudinal and cross-sectional study using advanced diffusion models and brain-age prediction. *Neuroimage.* 2021;224:117441. doi:10.1016/j.neuroimage.2020.117441
61. Ben-Shachar MS, Lüdecke D, Makowski D. Estimation of effect size indices and standardized parameters. *J Open Source Softw*. 2020;5(56):2815. doi:10.21105/joss.02815
62. Benjamini Y, Hochberg Y. Controlling the false discovery rate: a practical and powerful approach to multiple testing. *J R Stat Soc Series B: Stat Methodol.* 1995;57(1):289–300. doi:10.1111/j.2517-6161.1995.tb02031.x
63. Dziuban CD, Shirkey EC. When is a correlation matrix appropriate for factor analysis? Some decision rules. *Psychol Bull.* 1974;81:358–361. doi:10.1037/h0036316
64. Eikenes L, Visser E, Vangberg T, Håberg AK. Both brain size and biological sex contribute to variation in white matter microstructure in middle-aged healthy adults. *Hum Brain Mapp.* 2023;44(2):691–709. doi:10.1002/hbm.26093
65. Leroux E, Delcroix N, Dollfus S. Abnormalities of language pathways in schizophrenia patients with and without a lifetime history of auditory verbal hallucinations: a DTI-based tractography study. *World J Biol Psychiatry.* 2017;18(7):528–538. doi:10.1080/15622975.2016.1274053
66. Salisbury DF, Seebold D, Longenecker JM, Coffman BA, Yeh FC. White matter tracts differentially associated with auditory hallucinations in first-episode psychosis: a correlational tractography diffusion spectrum imaging study. *Schizophr Res.* 2023;265:4–13. doi:10.1016/j.schres.2023.06.001
67. Sagarwala R, Nasrallah HA. The effect of antipsychotic medications on white matter integrity in first-episode drug-naïve patients with psychosis: a review of DTI studies. *Asian J Psychiatry* 2021;61:102688. doi:10.1016/j.ajp.2021.102688
68. Wang Q, Cheung C, Deng W, *et al.* White-matter microstructure in previously drug-naive patients with schizophrenia after 6 weeks of treatment. *Psychol Med.* 2013;43(11):2301–2309. doi:10.1017/S0033291713000238
69. Zeng B, Ardekani BA, Tang Y, *et al.* Abnormal white matter microstructure in drug-naive first episode schizophrenia patients before and after eight weeks of antipsychotic treatment. *Schizophr Res.* 2016;172(1):1–8. doi:10.1016/j.schres.2016.01.051
70. Serpa MH, Doshi J, Erus G, *et al.* State-dependent microstructural white matter changes in drug-naïve patients with first-episode psychosis. *Psychol Med.* 2017;47(15):2613–2627. doi:10.1017/S0033291717001015
71. Ozcelik-Eroglu E, Ertugrul A, Oguz KK, Has AC, Karahan S, Yazici MK. Effect of clozapine on white matter integrity in patients with schizophrenia: a diffusion tensor imaging study. *Psychiatry Res.* 2014;223(3):226–235. doi:10.1016/j.pscychresns.2014.06.001
72. Beaulieu C. The basis of anisotropic water diffusion in the nervous system—a technical review. *NMR Biomed.* 2002;15(7–8):435–455. doi:10.1002/nbm.782
73. Jelescu IO, Palombo M, Bagnato F, Schilling KG. Challenges for biophysical modeling of microstructure. *J Neurosci Methods.* 2020;344:108861. doi:10.1016/j.jneumeth.2020.108861
74. Jones DK, Knösche TR, Turner R. White matter integrity, fiber count, and other fallacies: the do's and don'ts of diffusion MRI. *Neuroimage.* 2013;73:239–254. doi:10.1016/j.neuroimage.2012.06.081
75. Guglielmetti C, Veraart J, Roelant E, *et al.* Diffusion kurtosis imaging probes cortical alterations and white matter pathology following cuprizone induced demyelination and spontaneous remyelination. *Neuroimage.* 2016;125:363–377. doi:10.1016/j.neuroimage.2015.10.052
76. Song SK, Yoshino J, Le TQ, *et al.* Demyelination increases radial diffusivity in corpus callosum of mouse brain. *Neuroimage.* 2005;26(1):132–140. doi:10.1016/j.neuroimage.2005.01.028
77. Sun SW, Liang HF, Trinkaus K, Cross AH, Armstrong RC, Song SK. Noninvasive detection of cuprizone induced axonal damage and demyelination in the mouse corpus callosum. *Magn Reson Med.* 2006;55(2):302–308. doi:10.1002/mrm.20774
78. Winklewski PJ, Sabisz A, Naumczyk P, Jodzio K, Szurowska E, Szarmach A. Understanding the physiopathology behind axial and radial diffusivity changes—what do we know? *Front Neurol.* 2018;9:92. doi:10.3389/fneur.2018.00092

79. Seehaus A, Roebroeck A, Bastiani M, *et al.* Histological validation of high-resolution DTI in human post mortem tissue. *Front Neuroanat.* 2015;9:98. doi:10.3389/fnana.2015.00098
80. Palaniyappan L, Homan P, Alonso-Sanchez MF. Language network dysfunction and formal thought disorder in schizophrenia. *Schizophr Bull.* 2023;49(2):486–497. doi:10.1093/schbul/sbac159
81. Schmack K, Bosc M, Ott T, Sturgill JF, Kepecs A. Striatal dopamine mediates hallucination-like perception in mice. *Science.* 2021;372(6537):eabf4740. doi:10.1126/science.abf4740
82. Xi YB, Guo F, Li H, *et al.* The structural connectivity pathology of first-episode schizophrenia based on the cardinal symptom of auditory verbal hallucinations. *Psychiatry Res Neuroimaging*. 2016;257:25–30. doi:10.1016/j.pscychresns.2016.09.011
83. Catani M, Craig MC, Forkel SJ, *et al.* Altered integrity of perisylvian language pathways in schizophrenia: relationship to auditory hallucinations. *Biol Psychiatry.* 2011;70(12):1143–1150. doi:10.1016/j.biopsych.2011.06.013
84. Xie S, Liu B, Wang J, *et al.* Hyperconnectivity in perisylvian language pathways in schizophrenia with auditory verbal hallucinations: a multi-site diffusion MRI study. *Schizophr Res.* 2019;210:262–269. doi:10.1016/j.schres.2018.12.024
85. Figley CR, Uddin MN, Wong K, Kornelsen J, Puig J, Figley TD. Potential pitfalls of using fractional anisotropy, axial diffusivity, and radial diffusivity as biomarkers of cerebral white matter microstructure. *Front Neurosci*. 2022;15. https://www.frontiersin.org/articles/10.3389/fnins.2021.799576. Accessed January 25, 2023.